EXPLORING THE SOUND OF CHAOTIC OSCILLATORS VIA PARAMETER SPACES

Georg Essl

University of Wisconsin - Milwaukee
Milwaukee, Wisconsin, U.S.A.
essl@uwm.edu

ABSTRACT

Chaotic oscillators are exciting sources for sound production due to their simplicity in implementation combined with their rich sonic output. However, the richness comes with difficulty of control, which is paramount to both their detailed understanding and in live musical performance. In this paper, we propose perceptually-motivated parameter planes as a framework for studying the behavior of chaotic oscillators for musical use. Motivated by analysis via winding numbers, we extend traditional study of chaotic oscillators by using local features that are perceptually inspired. We illustrate the framework on the example of variations of the circle map. However, the framework is applicable for a wide range of sound synthesis algorithms with nontrivial parametric mappings.

1. INTRODUCTION

The use of nonlinear and chaotic oscillators for sound synthesis poses a trade-off. On the one hand, many of them have very simple algorithmic realizations and very diverse and rich sonic outcomes. On the other hand, the output becomes complex with increased nonlinearity. This complexity is often referred to as chaos and is characterized by drastic changes in output in response to minor parametric changes and a sensitivity to initial values. Because of their desirable properties, chaotic oscillators have repeatedly found their way into sound synthesis research and musical practices [1, 2, 3, 4, 5, 6, 7, 8, 9] and recently has found a renewed interest with in the context of live musical performance [10].

Despite this longstanding interest, there are a number of areas which are central to understanding chaotic oscillators for musical use which remain under-explored. Individual chaotic oscillators are usually studied on specific parameter examples [11] while making it difficult to predict outcomes under change of parameters. A large set of algorithms that exhibit chaotic oscillation exist [10], but their relationship is poorly, if at all, understood. This makes it difficult to chose oscillators with intention.

In live music performance, the ability of the musician to navigate the possibilities of the sound synthesis algorithm can be critical. This relationship of synthesis parameters to performer control is recognized as a central problem in musical instrument design known as the *mapping problem* [12]. However the mapping relationship in this case is complex, calling for strategies that support the performer's ability to have a sense of predictability of the performance choices made.

The purpose of this paper is to propose a framework for making the relationship of parametric choice and sonic outcome of chaotic oscillators accessible visually. More specifically, in this paper we propose perceptually motivated parametric planes (sometimes also called "atlases" [13]). These are parametric spaces which visualize features of the chaotic oscillator over a range of performance parameters. The visual space helps us understand dependence of parameters to outcomes, and the selection of features allows us to probe different aspect of the outcome potential.

2. RELATED WORK

Visualizations have long played an important role in the study of nonlinear oscillators. Perhaps closest to our proposed approach are two forms of visualization: (1) Arnold Tongues [14] and (2) Spectral Bifurcation Diagrams [15, 16].

Originally, Arnold tongues referred to stability regions of the circle map rendered as a plane with linear frequency Ω of the map as one coordinate, and increasing nonlinearity k as the other [14]. Since then, Arnold tongues have been more broadly referred to as regions of stability representing mode-locking in chaotic dynamical systems in general [17, 18, 19, 20, 13]. The literature discussing aspects of Arnold tongues is, in fact, so vast that it cannot be sensibly included here. The pervasiveness of this approach to studying nonlinear dynamics is one of the main motivations of using it as a starting point for our proposed approach. This should allow comparison to the vast existing body of research on nonlinear oscillators. Our proposed work can be understood to generalizing the parameter planes of Arnold tongue to depict behavior that is perceptually motivated in nature and in particular studies the use of spectral content.

Spectral Bifurcation Diagrams constitute another visualization approach for nonlinear phenomena proposed in the context of studying their acoustics [15, 16]. They are rendered by drawing the short-time spectrum of the iterative map with increasing iterative steps. Hence it is a method for depicting the onset of chaos over time within an oscillatory system. Our approach also uses spectral content. However, we are looking for different parametric relationships, and primarily those useful for control changes.

Within the realm of musical use of chaotic oscillators, this work is related to recent proposals to modify chaotic oscillators by injecting delay lines to make them more friendly to control by musical performers and the associated emergence of a large number of proposed nonlinear oscillators [10] . However, our understanding of the detailed aspects of the effect of delay lines to diverse nonlinear oscillators as well as the relationships and differences between these oscillators is currently preliminary. Our work looks to provide a concrete framework to study nonlinear oscillators for musical use and supplement their performance visually, hence is intended to help us systematically probe these open questions.

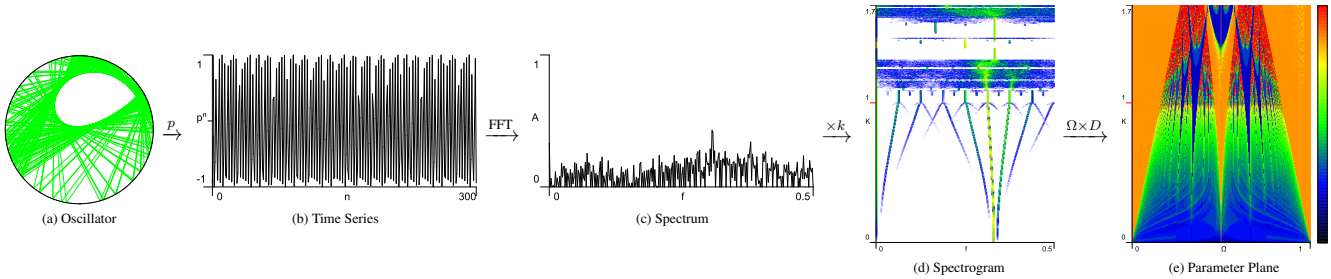

Figure 2: Visual representations of a nonlinear oscillator depicting intermediate steps of constructing parameter planes: (a) Circle Map as example of an iterative map, (b) projection of the map into a time series, (c) amplitude spectrum of the time series, (d) spectrogram of the time series over increased nonlinearity k with fixed linear frequency Ω, (e) parameter plane computing the PeakSparsity feature over a range of Ω.

3. CIRCLE MAPS AS NONLINEAR OSCILLATOR

While the proposed framework is not limited to a specific nonlinear oscillator, a concrete example will facilitate the discussion of the method. For this reason we will utilize circle maps [8, 11].

The most general form of circle maps refers to all mappings from the circle to itself [8]. Here we will restrict this to a perturbative form of the linear oscillator defined as follows:

$$y_{n+1} = \left(y_n + \Omega - \frac{k}{2\pi} f(y_n) \right) \mod 1 \tag{1}$$

Here $f(\cdot)$ refers to a nonconstant function that reflects a chosen type of nonlinearity. k is the strength of the nonlinearity. If k is 0 then the map is linear. Ω is a linear increment on the circle and reflects the distance traveled by a linear oscillator for one time step. y_n is the iterative position on the circle. y_0 is an initial value of the position. Technically the circle map hence has three parameters, Ω, k, and y_0. Finally the choice of the nonlinear function $f(\cdot)$ provides a further source of variation. One of the most widely studied circle map uses a sine function (equation (7)) as nonlinear perturbation and we will call this particular instance of the circle map the *sine circle map* [21]. In Figure 2(a) successive iterations of a sine circle map are connected by straight lines.

3.1. Choice of Projection

There is no set way to arrive at a time series from an iterative map such as the circle map. For our purpose, we follow [8] and define a *projection* $p(\cdot)$ onto an orthogonal axis:

$$p_n = \sin(2\pi y_n) \tag{2}$$

This choice of projection is justified because it mimics the projection used to construct a linear discrete sinusoidal oscillator from a phase function. In this case a constant increment Ω in the phase yields a sinusoidal output. Hence we can interpret the circle map equation (1) as an iterative nonlinear phase function, where Ω corresponds to the constant phase increase of a linear oscillator, and where k corresponds to the strength of a nonlinear contribution $f(\cdot)$ to phase change.

It is important to note that this choice of projection is arbitrary. One could use $\cos$ or in fact any other orthogonal projection of the circle for $p(\cdot)$. One could also simply interpret the y_n as time series. A wide range of further choices are also possible. We do believe that the $\sin$ is a natural choice as $y_0 = 0$ corresponds to a zero phase sinusoidal oscillation, and because it allows the interpretation of the circle map as a one-parameter nonlinear perturbation of a linear oscillator, hence grounding the map in a well-understood base configuration.

This particular justification is specific to this nonlinear dynamical system, and other dynamical systems may justify different projection functions.

4. PARAMETER PLANES AS FRAMEWORK FOR ANALYSIS

For the purpose of this paper we refer to *parameter planes* as two-dimensional visual renderings of behavior of a sound synthesis algorithm under the variation of two control parameters. This is different from other dense visual renderings such as a spectrogram, where typically the coordinate parameters are not necessarily directly related to control parameters, though the content of the visualization may well be responsive to parameter changes.

Assume any synthesis algorithm with two or more control parameters. The parameter plane would be the rendering along two control parameters (or combinations of control parameters that reduces their number to two). The local visual content is the output of the synthesis algorithm reduced by some feature process to a one-dimension that is then rendered as color gradient. Hence, parameter planes constitute the relationship of control parameter to some feature-specific output.

A pertinent established example of a parameter plane in the study of nonlinear oscillators are Arnold tongues. Arnold tongues are rendered by varying the two control parameters (Ω, k) of equation (1) or comparable comparable parameters of other nonlinear oscillators. The local feature traditionally used are winding numbers, which allow for the classification of the type of winding, and was used to discover mode-locking for mild nonlinearities in nonlinear oscillators [14].

Our proposed use of parameter planes can be understood as a generalization of Arnold tongue planes, but with the computation of the local value changed from the winding number to some other local feature of interest that is more suitable for understanding of audio properties.

The overall process through intermediary steps is depicted in Figure 2. We are given a nonlinear oscillator (Figure 2(a)). The choice of connecting the nonlinear oscillator to a time-series (Figure 2(b)) that is taken to be a sampled audio signal is not obvious. Hence we require a choice of function (*projection*) $p(\cdot)$ that establishes this relationship. Over a certain range of time-steps, we

compute local features. In our examples all newly introduced local features are spectral in nature, hence we compute the *FFT* (Figure 2(c)). It is important that this and the next step are flexible. One could choose a non-spectral feature (such as zero-crossings). In the spectral case, one can compute a further intermediary step of arranging a spectrogram over one control parameter (Figure 2(d)). This step is also not strictly required but we found it to be a very useful intermediate visualization to probe aspects of spectral evolution under parameter changes. Finally, a *feature mapping* $D(\cdot)$ derives from the spectrum a one-dimensional local representation that is arranged into the plane (Figure 2(e)) over the control parameter which we label here k and Ω for consistency with our chosen example of the circle map (section 3).

The specific aspects that are of interest for investigation and performance dictate further choices in this process. Oscillators can have initial transients. While these can be interesting subjects on their own right, for the purpose of this paper we have sought to capture steady state behavior. For this reason all figures in this paper, unless otherwise noted, compute the first 1000 iterations without consider them for rendering[1] The length of the time series, and the size of the FFT are further choices that can impact fidelity of the rendering and the information that will be drawn out. The following process was used to compute spectral information: A fast Fourier transform (FFT) was performed with a length of 8192 bins. Time series intervals were rendered for half that length and zero padded. The signal was weighted using a Blackman window function. Only the amplitude spectrum was considered. Neighboring bins were averaged to reduce the number of bins to the figure widths rendered in the paper (300 points). All aggregate feature computations were computed on the 300 bin averaged spectrum to create maximum relation between visual representations of spectra, spectrograms, and parameter planes. We do not propose this as a necessary aspect of the process. In other applications it may be desirable to compute feature on larger (or smaller number of bins).

Finally, a color gradient is chosen to render the one-dimensional feature D. This relationship can be linear or be further modified by a transfer function. It is common to use the logarithm on one-dimensional audio measures. In this paper all figures based on spectral information were color rendered on a logarithmic scale, normalized to the range of the color gradient.

Figure 2(e) shows the chosen color column to the right. The normalized color gradient ranged from zero to one and is composed of four equal intervals of length $1/4$. It is computed as linear interpolation of RGB colors black $(0, 0, 0)$, blue $(0, 0, 255)$, green $(0, 255, 0)$, yellow $(255, 255, 0)$, and red $(255, 0, 0)$. Hence black reflecting a value of 0, pure green reflecting a value of 0.5, and pure red reflecting a value of 1. For spectrogram computations we replaced black with white to achieve a white background look, with the color gradient otherwise unchanged.

Our Java implementation of the process for all features discussed in the next section took between 30 seconds to a few minutes depending primarily on the spectral window size used. In order to facilitate interactive use (for musical purposes or in interactive demonstration) we stored the resulting array of features in a file for instantaneous recall.

[1] 1000 was chosen after it was observed that this was sufficient to capture rare long transitions in parameter ranges of interest. The vast majority of transitions are very short and do not exceed just a few steps.

5. LOCAL FEATURES

A key component of computing parameter planes is finding local features that fill the plane to inform about the underlying behavior of the synthesis algorithm at a parameter point (Ω, K). The choice of this local feature carries reduces all of the behavior of the synthesis algorithm to a number, with the goal for this number to represent information of interest. By spanning a plane that allows one to inspect the evolution of local behavior under parameter change.

In order to understand that choice of feature we first discuss a widely established example in the study of nonlinear dynamical systems, which will motivate why we need more measures to study the sound of these systems.

5.1. Winding Numbers and Arnold Tongues

The construction of Arnold tongues is an example of a parameter plane visualization. Arnold tongues are areas in the parameter plane which exhibit mode locking [14, 17, 18, 22, 23] as well as provide a range of information about the transition into chaotic regimes. The *winding number* W (interchangably also referred to as rotation number [18]) is the local feature used for their construction. Given an iterator producing incremental states y_n, the winding number W is the average long-term map increment, hence describes the long-time average phase of the map. For iterations that are not subject to periodicity induced by modulo operations, they can be computed as [8]:

$$W = \lim_{n\to\infty} \frac{y_n - y_0}{n} \tag{3}$$

In practical computation the length of winding n is finite but sufficiently large to overcome initial transients. We chose 1000 for our depictions of Arnold tongues throughout this paper, matching our assumed maximum transients.

Computing the winding number over parameters of nonlinear oscillators led to the discovery of mode-locking (though phase-locking [24] is probably a more precise term in the case of the circle map). With mild increase in nonlinearity one finds that nonlinear oscillators tend to form areas of constant winding number even though the underlying parameters are changing. If depicted as a function of constant nonlinearity these form a staircase shape, which have been called "devil's staircase". When plotted over increasing nonlinearity, the family of devil's staircases widen, forming tongue-like shapes in the plane. We see depictions of Arnold tongues for the sine circle map in the bottom part of Figure 3(a). For low nonlinearity $k < 1$ we observe that widening regions of locked modes occur.

As we will see, Arnold tongue-like properties are very persistent features, even if we change the local feature we are computing. However, the winding number is still not a great feature to use to study sonic qualities of nonlinear dynamics. The winding number following equation (3) can be interpreted as a very-long-time averaged behavior of the state of the dynamical system. In fact, the equation can be formulated such that it is identical to the computation of the mean with the length of the mean being extended to infinity [24]. From this we observe that the winding number does not capture more localized properties of the dynamics, such as local periodicity, short-term spectral changes and so forth. Furthermore, given that we project the circle map into a discrete sine oscillator, giving us the interpretation of a phase function, we realize that the winding number here is really the long-term average

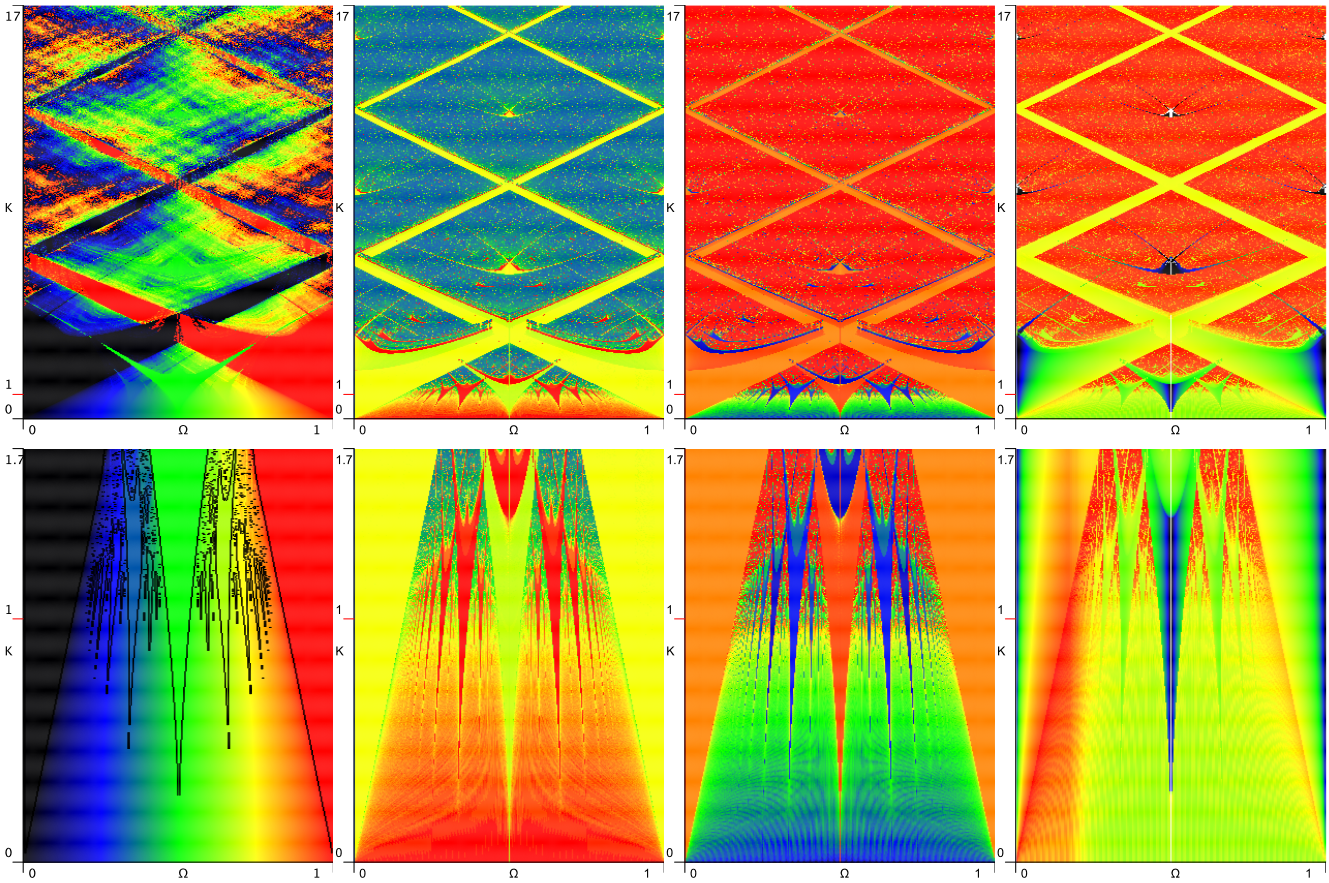

(a) Winding Number (b) MeanBalance (c) PeakSparsity (d) Entropy

Figure 3: Comparison of features computed in the parameter plane: (a) winding number (Arnold Tongues), (b) Spectral Mean Balance, (c) Spectral Peak Sparsity, (d) Spectral Entropy. (top) $k = [0, 13.\dot{3})$ (bottom) $k = [0, 1.3\dot{3})$ Arnold tongues use black contours to emphasize mode-locking transitions.

phase. While the precise response to phase in sound is a complicated phenomena, and it can play a role in specific settings [25], our ear generally does not associate perceptible qualities to phase. Hence a feature that primarily looks at phase is not the best feature to consider unless one is trying to capture very specific effects.

There are numerous aspects of iterative maps that could replace the winding number. For example, one can compute initial transient times by computing the winding number incrementally and checking when the computed winding numbers of successive steps fall below a value ϵ. The iteration count n then provides a measure of the duration of the transient. One can also probe for other mathematically interesting properties such as fixed points [11]. These would correspond to DC signals and help identify regions of silence, which is easily captured as part of richer and more broadly descriptive features.

5.2. Perceptually Motivated 1-D Features

Understanding the results of a synthesis algorithm is eminently perceptual, motivating the need for visual guidance of complex synthesis methods to predict perceptually interesting aspects of the expected sonic outcomes.

Perceptual cues are a particular form of features derived from audio time series. A wide array of audio features have been proposed [26] for they play important roles in all forms of audio analysis, including in creating meaningful starting points for machine classification. The body of audio features are dominated by needs of understanding human vocalization and musical signals. While nonlinear oscillators produce resonant spectra quite well suited by this body of work, especially at higher nonlinearities the sounds exhibit a range of differing noisy outcomes [11]. The literature dealing with noise is substantially smaller [27, 28]. This may go along with our understanding of human sound perception having substantially more detailed results for resonant spectral content than otherwise [29]. For the purpose of presenting the method, we were looking for features that would give clear visual differences over the same parameter space. After initial experimentation, we decided to present here three features that we believe to have a particular motivation given the output of nonlinear oscillators. Nonlinear oscillators have a range of effects: At low nonlinearities they tend to behave similar to wave shaping [8] in that the nonlinearity introduces spreading resonant spectra. At higher nonlinearity complicated noise-like patterns can emerge. Hence we were interested in features that could carry information about both resonant and noisy content.

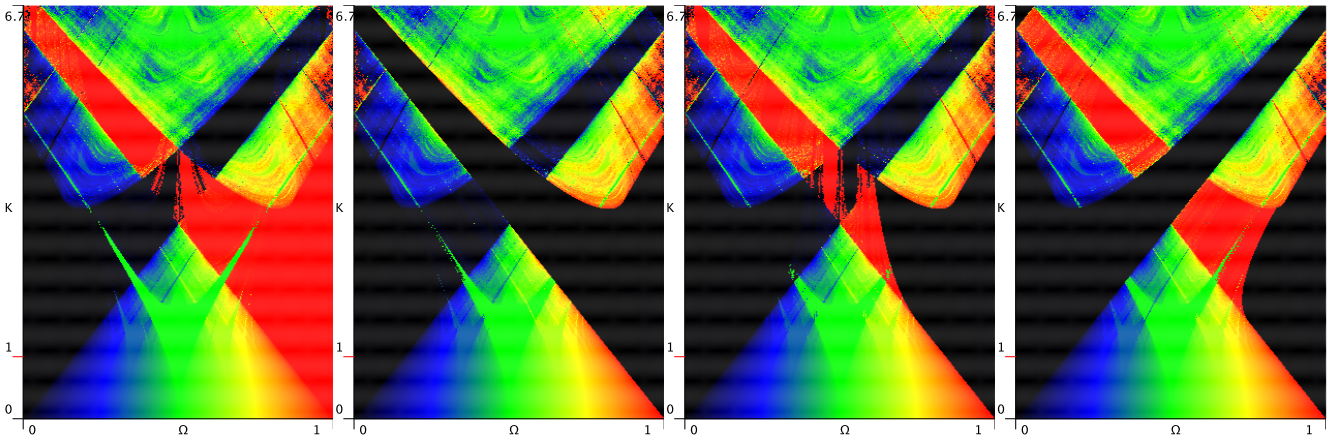

Figure 4: Arnold Tongues (winding numbers) of the sine circle map for initial values $y_0 = 0.0, 0.25, 0.5$, and 0.75.

5.2.1. *MeanBalance Feature*

The MeanBalance feature is quantifying if a spectrum is dominated by contributions that lie above or below the mean of the spectrum. The intuition is that a flat but noisy spectrum will be balanced with respect to the number of values that lie above and below the mean. For a spectrum of distinct and sparse narrow peaks, most values lie below the mean due to the sparsity of the peaks. A spectrum characterized that occasionally dips in the spectrum would, conversely, have most values lie above the mean. More precisely, the feature is computed as:

$$\text{mean} = \frac{1}{N}\sum_{n=1}^{N} f_n \qquad X[c] = \begin{cases} 0, & \text{if } c \text{ is false} \\ 1, & \text{otherwise} \end{cases}$$

$$b = \sum_{n=1}^{N} X[b > \text{mean}] \qquad a = \sum_{n=1}^{N} X[b < \text{mean}]$$

$$D_{\text{MB}} = \begin{cases} b/a & \text{if } a > 0 \\ 1 & \text{if } a = 0 \text{ and } b = 0 \\ b & \text{otherwise} \end{cases} \tag{4}$$

mean is the customary mean over all FFT bins f_n. b is the count of FFT bins that lie below the mean of the spectrum, and a is the count of FFT bins above the mean of the spectrum. If $a = 0$, we define $D_{\text{MB}} = b$. If all bins are equal to the mean $D_{\text{MB}} = 1$.

We expect D_{MB} to return high values for sparse peak spectra, return average values for flat spectra, and return low values for spectra with occasionally dips.

5.2.2. *PeakSparsity Feature*

The PeakSparsity feature takes an integral approach to estimating how peak-dominated a spectrum is. The core idea is that the area underneath the spectrum, characterized by the mean, can be arrived at in various ways. If the spectrum is peaky, we expect that there is more area under a peak. Hence high peaks will occupy more of the area than a flat spectrum. The spectrum sorts the peaks in the spectrum and then counts how many sorted bins are needed to arrive at the mean. If lots of area in within a few very high peaks it will take only a few bins to reach the mean. If the spectrum is flat, we expect to have to count all bins to arrive the mean. Hence PeakSparsity is a measure of sparsity peaks in the spectrum. It is computed as follows:

$$\text{area}_n = \sum_{m=1}^{n} \text{sort}_m(f) \qquad \text{sort}_n(f) \text{ are sorted FFT bins}$$

$$\text{c}_n = \begin{cases} 1 & \text{if } \sum_{m=1}^{n} \text{area}_m \leq \text{mean} \\ 0 & \text{otherwise} \end{cases}$$

$$D_{\text{PS}} = \sum_{n=1}^{N} c_n \tag{5}$$

5.2.3. *Spectral Entropy Feature*

Spectral entropy [27] is the computation of the Shannon entropy over all FFT bins:

$$D_{\text{Ent}} = -\frac{1}{\log N}\sum_{n=1}^{N} f_n \log(f_n) \tag{6}$$

f_n are the FFT bins and N is the number of bins up to half Nyquist frequency. Description by Shannon entropy leads to information-theoretic interpretation of the measure. High entropy corresponds to the requirement to describe more information content. Hence it is a kind of measure of information-theoretic complexity of the spectrum. We expect sparse spectra to contain less information than dense spectra, but per chance have some information-theoretic differentiation between different forms of dense spectra.

6. PARAMETER SPACES FOR CIRCLE MAPS

We are now ready to proceed to give concrete illustrations of parameter planes using these chosen features on variations of the circle maps introduced in section 3.

6.1. Comparisons of features

Figure 3 compares different choices of local features computed in the (Ω, k) parameter plane for the sine circle map. The figure shows both a weak nonlinearity regime ($k \in [0, 1.7)$) in the bottom row as well as a strong nonlinearity region ($k \in [0, 17)$) in

the top column. We include the winding number as classical local feature on the left.

Mild nonlinearity: Each of the four illustrated features highlight very different structures in the very low nonlinearity regime $k \in [0, 0.3)$. The winding number does not show the emerging resonant spectral aspects that emerge in this region. Specifically the PeakSparsity feature shows an overall increase in resonant peaks with additional fine structure. While Entropy displays a different structure than any other feature it shares with the winding number the lack of detail in this very mild nonlinearity regime.

nonlinearity near invertibility: The sine circle map becomes non-invertible at $k \geq 1$ [8]. This point is marked on the k-axis with a red marker. We expect more pronounced nonlinear effects to occur after this point, and early cascades into chaos are possible. Overall we see that both the MeanBalance and the PeakSparsity measure show substantial fine structure in the region $k \in [1, 1.3\dot{3})$. While the winding number exhibits a lot of structure it does not align well with these transitional properties. Entropy shows little change until chaos onset, when we see a smooth transition.

Persistent macroscopic properties and their variation: Arnold Tongue shapes are visible with all chosen features which make them very robust properties. This means that they do not merely correspond to mode-locking, but also have spectral and entropic effects. Unsurprisingly, fixed point regions (crossing diagonal regions) can be identified with all features as they correspond to constant value, and DC component spectral content. It is noteworthy however that the Entropy feature provides additional information in fixed point regions because it differentiates information content by the level of the DC component. These feature as not perceptually relevant, suggesting that unmodified entropy may not be an ideal feature for perceptually motivated modeling.

Strong nonlinearity: For a parameter range of $k \gg 1$ chaotic behavior, potentially interspersed with fixed-point regions, that then re-cascade into chaos, are dominating the behavior of the sine circle map for all features. Here the winding number presents the most diversity in value ranges, but is poor at resolving some visible trends that emerge using the other features. There are some subtle differences which of these trends are highlighted how strongly between MeanBalance, PeakSparsity and Entropy. For example using Entropy we see trend lines at the half-way point between fixed point diagonal regions. MeanBalance shows more structure that follows central fixed point and stability regions around $\Omega = 0.5$.

6.2. Initial Value Sensitivity

As illustrated on a number of examples [11], the circle map exhibits initial value sensitivity, a feature that is known to be typical of chaotic systems, and a widely propagated narrative in popular culture involving butterfly wings. While known examples [11] make clear that observable and clearly perceptible differences due to initial value differences can occur through the parameter plane, inspection of the parameter plane allows us to look for initial value effects more broadly. Arnold Tongues exhibit initial value sensitivity as discernible differences in the plane, in particular in areas that approach recurrent chaotic regimes, as well as in the behavior of crossing fixed point regions.

Figure 4 exhibits this effect. We see that for increasing initial values, certain regions change. With respect to fixed point regions, we see that for initial values below 0.5, one side overlaps the other, while this directionality is flipped for initial values above 0.5.

In order to understand if these differences are perceptually relevant, we observe initial value conditions on a perceptual feature instead of the winding numbers used in Arnold tongues (Figure 3). We see that the features at the top end of fixed point diagonals in the winding number plane is not captured by any of the other measures. Some of these effects can perceptually be treated as phase effects and hence are not usually perceptually relevant. Mathematically they do not appear in our features due to using only the amplitude spectrum.

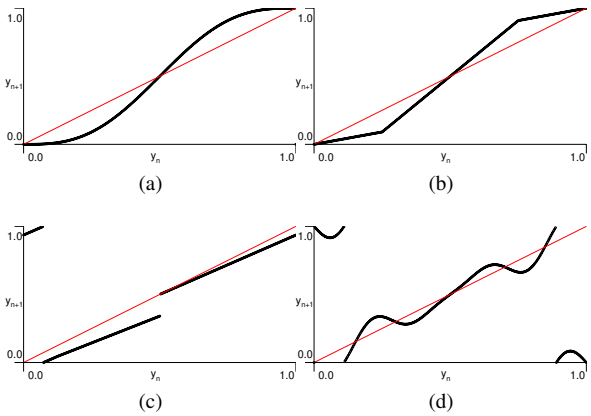

Figure 5: Four nonlinearities functions explored: (a) Sine, (b) Triangle, (c) Piecewise linear cardiorespiratory coupling model [20], (d) truncated Fourier-series. Figure from [11].

7. VARIATION OF NONLINEAR FUNCTION

To explore the impact of the variation of the nonlinear function $f(\cdot)$ we use four exemplar functions discussed in [11]:

$$f(y_n) = \sin(2\pi y_n) \tag{7}$$

$$f(y_n) = \begin{cases} 4 \cdot y_n & \text{if } 0 \leq y_n < 1/4 \\ (1/4 - y_n) \cdot 4 + 1 & \text{if } 1/4 \leq y_n < 3/4 \\ (y_n - 3/4) \cdot 4 - 1 & \text{otherwise.} \end{cases} \tag{8}$$

$$f(y_n) = \begin{cases} \frac{y_n + T}{1 + 2 \cdot \epsilon \cdot T} & \text{if } 0 \leq y_n < B \\ \frac{y_n + (1 - 2 \cdot ep) \cdot T}{1 - 2 \cdot \epsilon \cdot T} & \text{if } b \leq y_n < 1 - T \\ \frac{y_n + T - 1}{1 + 2 \cdot \epsilon \cdot T} & \text{if } 1 - T \leq y_n \leq B + 1 \\ \frac{y_n + (1 - 2 \cdot \epsilon) \cdot T - 1}{1 - 2 * \epsilon \cdot T} & \text{otherwise.} \end{cases} \tag{9}$$

$$f(y_n) = \frac{1}{A} \sum_{m=1}^{4} a_m \sin(2\pi m y_n) \tag{10}$$

With $T = 0.5$, $\epsilon = 0.25$ and $B = 0.5 + (\epsilon - 1) \cdot T$ in (9) and with $a_m = \{1, \frac{1}{2^2}, \frac{1}{3^2}, \frac{1}{4^2}\}$ and $A = a1 + a2 + a3 + a4$ in (10). Equation (8) is a triangle function. Equation (9) is a piecewise linear function from the biomedical literature [20] and equation (10) is a Fourier-series composition with four terms. The functions are shown in Figure 5. The variation of nonlinear function is depicted in Figure 6 using the PeakSparsity feature. Obviously the variation of the nonlinear function has substantial large scale impact on the response, though Arnold tongue-like features are persistent in all cases. For the continuous piecewise linear (triangle) function, we observe a well-known effect of tongues pinching together with increase nonlinearity. This effect has been called "Sausages" [30].

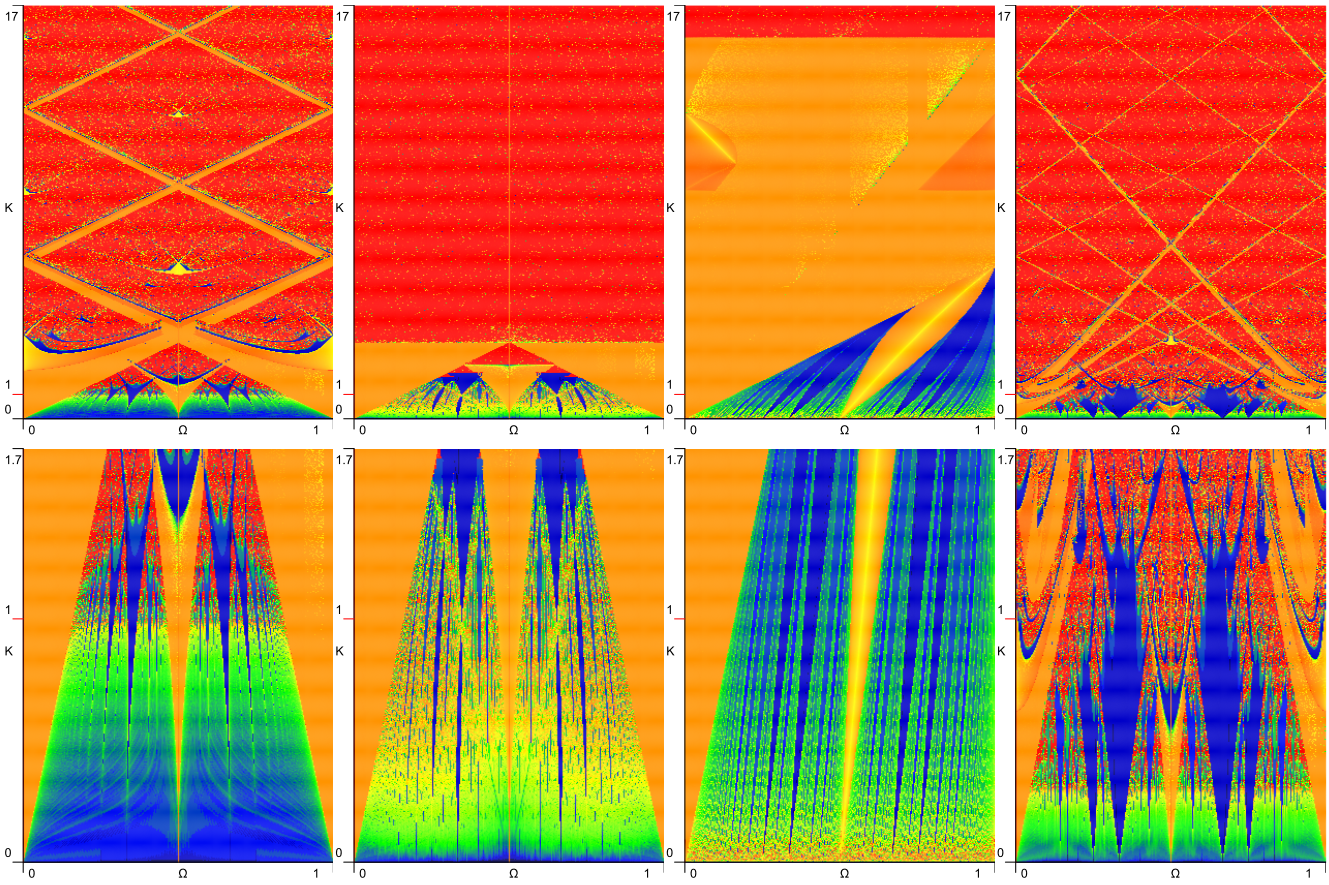

(a) Sine (b) Triangle (c) Cardiorespiratory (d) Fourier

Figure 6: Variation of nonlinear perturbation function in the circle map using the PeakSparsity spectral value in the (k,Ω)-plane (top) mild nonlinearity with $k \in [0, 1.3\dot{3})$ (bottom) strong nonlinearity with $k \in [0, 13.\dot{3})$ (a) sine, (b) continuous rectilinear, (c) discontinuous rectilinear, (d) mixed three sine.

The asymmetric non-continuous piecewise linear case (cardiorespiratory model) shows that symmetry can be broken as well as that fixed point regions can be very substantially extended. Some of this behavior can be explained by understanding occurance of fixed points by the slope of the function against an intersection with the identity map $y_n = y_{n+1}$ depicted in Figure 5 as a red diagonal line. If the angle is shallow it creates fixed points. For the triangle case we observe no fixed points due to the choice of slope, while in the cardiorespiratory case we see an abundance of fixed points for the choice of slope and intersection with the identity.

Overall we note that while there are persistent structure between nonlinear function, the choice of nonlinearity plays a substantial role in the sound of a chaotic oscillator. This suggests that the study of their variation is an interesting subject of further investigation.

8. CONCLUSIONS

The study of chaotic oscillators is an extremely rich topic ripe for long-standing research. The proposed framework described in this paper offers a strategy to further our understanding of their behavior for sound synthesis.

The present framework is applicable to many more cases than the ones discussed in this paper. A comparative analysis of wave shaping, modulation techniques, feedback, and circle maps is forthcoming [31]. Yet a detailed study on a wide range of chaotic oscillators [10] would help crystallize criteria for picking algorithms and their respective similarities and differences.

The parameter space itself could be subjected to further analysis. For example, similarity measures [32] could be applied to related different points and regions in the parameter plane and hence provides a form of reparametrization that replaces parametric closeness with perceptual closeness.

Finally feature discovery and a deeper understanding of the perception of differing noisy sounds are key aspects that can help us get further understanding of nonlinear oscillators. We see the use of feature discovery by maximum discrimination as a promising strategy for detailed study of existing features [33] and also as a possible pathway towards understanding what aspects of the signal are poorly captured by the current feature landscape. Deepening our understanding of perception of noise is less straightforward and will require new perceptual experimentation with novel models ideas about what could constitute perceptually relevant mechanisms that discriminate difference versions of noise.

9. REFERENCES

[1] A. Di Scipio, "Composition by exploration of non-linear dynamic systems," in *Proceedings of the International Computer Music Conference*, 1990, pp. 324–327.

[2] B. Truax, "Chaotic non-linear systems and digital synthesis: an exploratory study," in *Proceedings of the International Computer Music Conference*, 1990, pp. 100–103.

[3] M. Gogins, "Iterated functions systems music," *Computer Music Journal*, vol. 15, no. 1, pp. 40–48, 1991.

[4] R. Bidlack, "Chaotic systems as simple (but complex) compositional algorithms," *Computer Music Journal*, vol. 16, no. 3, pp. 33–47, 1992.

[5] J. Mackenzie and M. Sandler, "Modelling sound with chaos," in *Proceedings of IEEE International Symposium on Circuits and Systems - ISCAS '94*, May 1994, pp. 93–96.

[6] R. Dobson and J. Fitch, "Experiments with chaotic oscillators," in *Proceedings of the International Computer Music Conference*, Banff, Canada, 1995, pp. 45–48.

[7] D. Slater, "Chaotic sound synthesis," *Computer Music Journal*, vol. 22, no. 2, pp. 12–19, 1998.

[8] G. Essl, "Circle maps as a simple oscillators for complex behavior: I. Basics," in *Proceedings of the International Computer Music Conference (ICMC)*, New Orleans, November 2006.

[9] R. Holopainen, *Self-organised sound with autonomous instruments: Aesthetics and experiments*, Ph.D. thesis, University of Oslo, 2012.

[10] E. Berdahl, E. Sheffield, A. Pfalz, and A. T. Marasco, "Widening the razor-thin edge of chaos into a musical highway: Connecting chaotic maps to digital waveguides," in *Proceedings of the International Conference on New Interfaces for Musical Expression*, L. Dahl, D. Bowman, and T. Martin, Eds., Blacksburg, Virginia, USA, June 2018, pp. 390–393, Virginia Tech.

[11] G. Essl, "Circle maps as a simple oscillators for complex behavior: II. Experiments," in *Proceedings of the International Conference on Digital Audio Effects (DAFx)*, Montreal, September 18-20 2006.

[12] E. R. Miranda and M. Wanderley, *New Digital Musical Instruments: Control And Interaction Beyond the Keyboard (Computer Music and Digital Audio Series)*, A-R Editions, Inc., Madison, WI, USA, 2006.

[13] S. P. Kuznetsov et al., "Two-parameter analysis of nonlinear systems. atlas of charts of dynamical regimes," `http://www.sgtnd.narod.ru/science/atlas/eng/`, Accessed: 2019-03-24.

[14] V. I. Arnold, "Small denominators, I: mappings of the circumference into itself," *Am. Math. Soc. Transl. (2)*, vol. 46, pp. 213–284, 1965.

[15] W. Lauterborn and E. Cramer, "Subharmonic route to chaos observed in acoustics," *Phys. Rev. Lett.*, vol. 47, pp. 1445–1448, Nov 1981.

[16] W. Lauterborn and E. Suchla, "Bifurcation superstructure in a model of acoustic turbulence," *Phys. Rev. Lett.*, vol. 53, pp. 2304–2307, Dec 1984.

[17] H. Mori, G.C. Paquette, and Y. Kuramoto, *Dissipative Structures and Chaos*, Springer Berlin Heidelberg, 2nd edition, 1998.

[18] J. M. T. Thompson and H. B. Stewart, *Nonlinear Dynamics and Chaos*, Wiley, 2nd edition, 2002.

[19] AP Kuznetsov, LV Turukina, AV Savin, IR Sataev, JV Sedova, and SV Milovanov, "Multi-parameter picture of transition to chaos," *Izvestija Vuzov. Applied Nonlinear Dynamics*, vol. 10, no. 3, pp. 80, 2002.

[20] M. McGuinness and Y. Hong, "Arnold Tongues in Human Cardiorespiratory Systems," *Chaos*, vol. 14, no. 1, pp. 1–6, 2004.

[21] Bai-Lin Hao and Wei-Mou Zheng, *Applied symbolic dynamics and chaos*, World scientific, 2nd edition, 2018.

[22] N. Y. Ivankov and S. Kuznetsov, "Complex periodic orbits, renormalization, and scaling for quasiperiodic golden-mean transition to chaos," *Physical review. E, Statistical, nonlinear, and soft matter physics*, vol. 63, pp. 046210, 05 2001.

[23] V. S. Anishchenko, V. Astakhov, A. Neiman, T. Vadivasova, and L. Schimansky-Geier, *Nonlinear Dynamics of Chaotic and Stochastic Systems: Tutorial and Modern Developments (Springer Series in Synergetics)*, Springer-Verlag, Berlin, Heidelberg, second edition, 2007.

[24] L. Glass and J. Sun, "Periodic forcing of a limit-cycle oscillator: Fixed points, arnold tongues, and the global organization of bifurcations," *Physical Review E*, vol. 50, no. 6, pp. 5077, 1994.

[25] O. Santala, *Perception and auditory modeling of spatially complex sound scenarios*, Ph.D. thesis, Aalto University, 2015.

[26] F. Alías, J. Socoró, and X. Sevillano, "A review of physical and perceptual feature extraction techniques for speech, music and environmental sounds," *Applied Sciences*, vol. 6, no. 5, pp. 143, May 2016.

[27] F. Alías and J. C. Socoró, "Description of anomalous noise events for reliable dynamic traffic noise mapping in real-life urban and suburban soundscapes," *Applied Sciences*, vol. 7, no. 2, pp. 146, 2017.

[28] X. Sevillano, J. C. Socoró, F. Alías, et al., "Dynamap–development of low cost sensors networks for real time noise mapping," *Noise Mapping*, vol. 3, no. 1, 2016.

[29] B.C.J. Moore, *Introduction to the Psychology of Hearing*, Academic Press, 4th ed. edition, 1995.

[30] W.-M. Yang and Hao B.-L., "How the arnold tongues become sausages in a piecewise linear circle map," *Communications in Theoretical Physics*, vol. 8, no. 1, pp. 1–15, jul 1987.

[31] G. Essl, "Connecting Circle Maps, Waveshaping, and Phase Modulation via Iterative Phase Functions and Projections," in *Proceedings of the 14th International Symposium on Computer Music Multidisciplinary Research (CMMR)*, 2019.

[32] J.-J. Aucouturier, F. Pachet, et al., "Music similarity measures: What's the use?," in *Proceedings of ISMIR*, 2002, pp. 13–17.

[33] T. Jebara and T. Jaakkola, "Feature selection and dualities in maximum entropy discrimination," in *Proceedings of the Sixteenth conference on Uncertainty in artificial intelligence*. Morgan Kaufmann Publishers Inc., 2000, pp. 291–300.